Soluble Oligomers of the Intramembrane Serine Protease YqgP Are Catalytically Active in the Absence of Detergents[†]

Xiaojun Lei,[‡,§] Kwangwook Ahn,[‡] Lei Zhu,[‡] Iban Ubarretxena-Belandia,[||] and Yue-Ming Li*[,‡,§]

Molecular Pharmacology and Chemistry Program, Memorial Sloan Kettering Cancer Center, New York, New York 10021, Department of Pharmacology, Joan Weill Graduate School of Medical Science of Cornell University, New York, New York 10021, and Department of Structural and Chemical Biology, Mount Sinai School of Medicine, New York, New York 10029

Received March 5, 2008; Revised Manuscript Received September 15, 2008

ABSTRACT: Rhomboid, a polytopic membrane serine protease, represents a unique class of proteases that cleave substrates within the transmembrane domain. Elucidating the mechanism of this extraordinary catalysis comes with inherent challenges related to membrane-associated peptide hydrolysis. Here we established a system that allows expression and isolation of YqgP, a rhomboid homologue from *Bacillus subtilis*, as a soluble protein. Intriguingly, soluble YqgP is able to specifically cleave a peptide substrate that contains the transmembrane domain of Spitz. Mutation of the catalytic dyad abolished protease activity, and substitution of another highly conserved residue, Asn241, with Ala or Asp significantly reduced the catalytic efficiency of YqgP. We have identified the cleavage site that resides in the middle of the transmembrane domain of Spitz. Replacement of two residues that contribute to the scissile bond by Ala did not eliminate cleavage, but rather led to additional or alternative cleavages. Moreover, we have demonstrated that soluble YqgP exists as oligomers that are required for catalytic activity. These results suggest that soluble oligomers of maltose binding protein−YqgP complexes form micellelike structures that are able to retain the active conformation of the protease for catalysis. Therefore, this work not only provides a unique system for elucidating the reaction mechanism of rhomboid but also will facilitate the characterization of other intramembrane proteases as well as non-protease membrane proteins.

Intramembrane proteases have emerged as a new class of membrane proteins, in which the catalytic residues of the protease reside within predicted transmembrane domains (*1, 2*). Moreover, the scissile bond of substrates appears to be situated within a transmembrane domain as well. Three classes of intramembrane protease have been reported: (1) S2P-type metalloprotease that processes the transcription factor SREBP (the sterol regulatory element-binding protein) (*3*), (2) presenilin/γ-secretase and signal peptide peptidase-type aspartyl proteases that cleave multiple substrates with broad biological activities (*4*−*6*), and (3) rhomboid-type serine proteases that activate Spitz, a transmembrane ligand for the EGF receptor in *Drosophila* (*7*). Intramembrane proteases play an important role in many physiological processes, such as cellular differentiation, lipid metabolism, protein folding, and virus infection (*8*). Elucidating the catalytic mechanism of intramembrane proteases has been a formidable challenge that requires novel approaches for dealing with membrane-associated enzymology, such as how to present an exogenous substrate to the protease and how to catalyze peptide hydrolysis in hydrophobic environments.

Rhomboid-1 (Rho-1) was the first rhomboid discovered through a genetic screen in *Drosophila*, and loss of function of Rho-1 leads to the formation of a pointed head in the embryonic skeleton (*9*). Rho-1 and another membrane protein, Star, have been genetically linked with EGF receptor signaling in *Drosophila* through the release of a transmembrane ligand, Spitz (*10*). Rho-1, a polytopic membrane protein, has been shown to be a serine protease which converts inactive Spitz into its active form (*7*). Star acts as a chaperone protein that escorts the inactive Spitz precursor from the endoplasmic reticulum to the Golgi where Rho-1 cleaves Spitz to release the active form. Rhomboid is widely conserved in all organisms (*11*). Additional functions of rhomboid-like proteins include quorum sensing in bacteria, host invasion by parasites, mitochondrial remodeling, and apoptosis in eukaryotic cells (*12*−*16*). The majority of examined rhomboids from mammals to bacteria are able to process Spitz. Recently, rhomboids have been biochemically reconstituted using purified recombinant protein (*17, 18*). These studies demonstrated that rhomboid is sufficient for exhibiting protease activity, which is distinct from γ-secretase that is active as a macromolecular complex. Lately, crystal structures of rhomboids from *Escherichia coli* and *Haemophilus influenzae* have been resolved (*19*−*22*). Structural studies have provided critical insights into the architecture

[†] This work is supported by NIH Grant AG026660 (Y.-M.L.), the Alzheimer's Association (Zenith Fellows Award to Y.-M.L.), and the American Health Assistance Foundation (Y.-M.L.). I.U.-B. was supported by National Science Foundation Grant MCB-0546087.

* To whom correspondence should be addressed: Molecular Pharmacology and Chemistry Program, Memorial Sloan Kettering Cancer Center, 1275 York Ave., New York, NY 10065. Telephone: (646) 888-2193. Fax: (646) 422-0640. E-mail: liy2@mskcc.org.

[‡] Memorial Sloan Kettering Cancer Center.

[§] Joan Weill Graduate School of Medical Science of Cornell University.

[||] Mount Sinai School of Medicine.

10.1021/bi800385r CCC: $40.75
Published on Web 10/21/2008

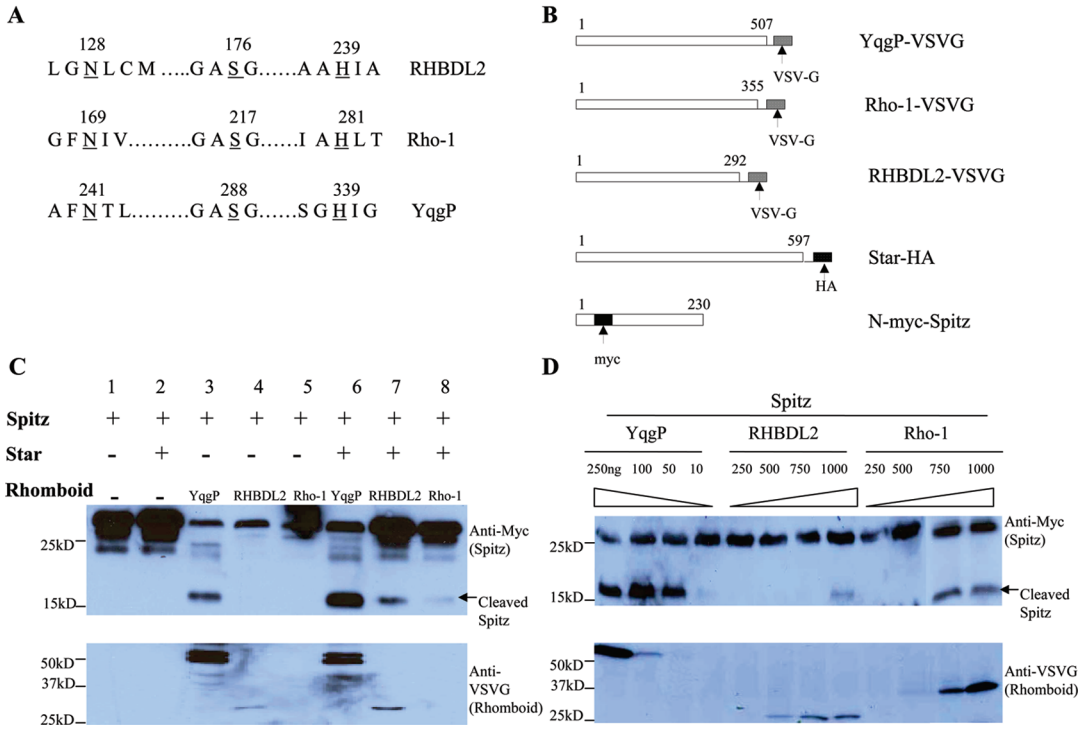

FIGURE 1: High levels of rhomboid are able to cleave Spitz in a manner independent of Star expression. (A) Amino acid alignment of rhomboid sequences that contain the catalytic dyad (S-H) and a conserved Asn from different species: RHBDL2, *Homo sapiens*; Rho-1, *Drosophila*; YqgP, *B. subtilis*. The catalytic key residues are indicated by underlined amino acids. (B) Schematic representation of constructs used in this study. All rhomboids were tagged on the C-terminus with VSV-G. Star was tagged with HA on the C-terminus, and a Myc tag was inserted between residues 80 and 81 of Spitz. (C) Spitz cleavage was Star-independent in proteolytic reconstitution in mammalian cell lines. COS-1 cells were transiently transfected with Myc-tagged Spitz, Star, and VSV-G-tagged rhomboids: (top) full-length Spitz (26 kDa) and its rhomboid-cleaved form (16 kDa) detected with anti-myc and (bottom) overexpression levels of rhomboids evaluated with anti-VSV-G. (D) Effect of expression levels of rhomboid on Spitz cleavage. Plasmid pCDNA3.1-YqgP was titrated down, while those of pcDNA3.1-RHBDL2 and Rho-1 were titrated up.

of the catalytic center, including the Ser-His dyad and the oxyanion hole for substrate binding and intramembrane proteolysis. Moreover, there is a gating mechanism that controls the entry of substrate into the hydrophobic active site. However, which protein domain functions as the gate remains a controversial matter. In addition, stable trimers or multimers of rhomboid have been observed, and their function is unknown (*18, 20*). The precise reaction mechanism of the rhomboid protease remains to be elucidated. Developing a system that enables determination of the kinetic parameters of rhomboid will facilitate the dissection of the reaction mechanism for substrate binding, catalysis, and specificity of rhomboids and will provide the molecular basis for structural and functional studies as well as for designing mechanism-based inhibitors.

In this study, we overexpressed and purified full-length YqgP, a rhomboid homologue from *Bacillus subtilis*, fused with maltose binding protein (MBP)[1] at the N-terminus (MBP−YqgP). Strikingly, MBP−YqgP can be isolated as a soluble protein in the absence of any detergent. More importantly, soluble MBP−YqgP is able to cleave a substrate that contains the transmembrane domain of Spitz without reconstitution into a lipid or detergent system. Biochemical and biophysical studies suggest that MBP−YqgP oligomerizes into complexes that mimic the micellelike environment and permit catalysis. Moreover, mutagenic, kinetic, and inhibitor analyses have shown that the activity of recombinant MBP−YqgP exhibits the characteristics of rhomboid as seen in cellular studies and YqgP isolated from membrane fractions.

EXPERIMENTAL PROCEDURES

Cell Lines and Reagents. Genomic DNA of *B. subtilis* and COS-1 were obtained from American type Culture Collection (ATCC). DH5α and BL21(DE3) strains were purchased from Invitrogen. Plasmids pcDNA3.1-Rhomboid-1, pcDNA3.1-Star, pcDNA3.1-RHBDL2, and pcDNA3.1-Spitz were kindly provided by M. Freeman of the MRC Laboratory of Molecular Biology. The following antibodies were used in the study: mouse monoclonal antibodies 9E10 against the Myc epitope (Monoclonal antibody facility, Memorial Sloan Kettering Cancer Center) and mouse monoclonal antibodies against β-tubulin, HA, and VSV-G (Roche Diagnostics, Indianapolis, IN).

Plasmid Constructs. All constructs used for mammalian transfection were built in pCDNA3.1. A Myc tag was introduced into pCDNA3.1-Spitz between residues 80 and 81. Three rhomboids (Rho-1, RHBDL2, and YqgP) were fused with the VSV-G tag (peptide sequence, YTDIEMNRLGK) on the C-terminus (Figure 1B). Plasmid pIAD16-YqgP was generated by inserting the YqgP gene into

[1] Abbreviations: CHAPS, 3-[(3-cholamidopropyl)dimethylammonio]-1-propanesulfonate; CHAPSO, 3-[(3-cholamidopropyl)dimethylammonio]-2-hydroxy-1-propanesulfonate; DCI, 3,4-dichloroisocoumarin; DDM, dodecyl β-D-maltoside; DFP, diisopropyl fluorophosphate; MBP, maltose binding protein; MCA, *N*-ε-[(7-methoxycoumarin-4-yl)acetyl]; PMSF, phenylmethanesulfonyl fluoride; SD, standard deviation; S2P, site 2 protease; TLCK, tosyl lysyl chloromethyl ketone; TMD, transmembrane domain; TPCK, tosyl phenylalanyl chloromethyl ketone.

bacterial expression vector pIAD16 (*23*) using the *Nde*I and *Hin*dIII restriction sites with the MBP tag at the N-terminus. The QuikChange site-directed mutagenesis kit (Stratagene) was used to generate mutated constructs.

Peptide Synthesis. All peptides in this study were synthesized using standard Fmoc solid-phase chemistry on a peptide synthesizer (Protein Technologies, Inc.). The same method was used to incorporate Fmoc-protected (MCA)-K {*N*-ε-[(7-methoxycoumarin-4-yl)acetyl]-L-lysine}, a fluorescent amino acid, into substrate peptides. All peptides were purified by high-pressure liquid chromatography (HPLC) on a reverse-phase C18 column. The identity of the peptides was verified by LC-MS/MS (Agilent Technologies).

Cell Culture, Transfection, and Lysate Preparation. COS-1 cells were grown in high-glucose Dulbecco's modified Eagle's medium (DME) supplemented with 10% fetal bovine serum, 100 units/mL penicillin, and 100 μg/mL streptomycin. Transfection was conducted in six-well plates with FuGENE 6 transfection reagent (Roche Diagnostics) according to the manufacturer's protocol. The cells were incubated at 37 °C for 48 h and then washed with cold PBS three times before being scraped off the plate. Cell pellets were lysed with RIPA buffer [50 mM Tris-HCl (pH 7.4), 1% NP-40, 0.25% sodium deoxycholate, 150 mM NaCl, and 0.1% SDS], 1 mM EDTA, 2 mM DTT, and protease inhibitor cocktail (Roche Diagnostics).

Overexpression and Purification of YqgP. Plasmid pIAD16-YqgP was transformed into the BL21(DE3) cells for protein expression. When bacteria cells reached an OD_{600} of 0.8, IPTG at a final concentration of 0.1 mM was added to induce the expression of the target protein at 20 °C for 5 h. Cell pellets that were resuspended in buffer A [20 mM Tris and 200 mM NaCl (pH 7.5)] were broken with a French press (Spectronic Instruments, Rochester, NY). Cell lysates were centrifuged at 10000*g* for 45 min. The supernatants then were centrifuged at 100000*g* for 60 min. The ensuing supernatant was applied to the amylose column and eluted with a gradient of buffer A containing 10 mM maltose. The eluted proteins were analyzed by SDS−PAGE and pooled for studies. In addition, we solubilized and purified the YqgP protein from membrane fractions by following the same procedure as described previously (*18*). The identity of YqgP proteins was confirmed by trypsin digestion and LC−MS/MS analysis.

In Vitro Cleavage Assay and Cleavage Site Mapping. The recombinant MBP−YqgP (15 μg) was incubated with 2 μM peptide substrate in 100 μL of assay buffer [50 mM PIPES (pH 7.0) and 4 mM DTT] at 37 °C for 3 h. The reaction was stopped by adding 5 μL of 5% TFA in water and centrifuged at 10000*g* for 10 min. Internal fluorescent standard MCA was spiked in each reaction mixture for calculation and normalization of the cleaved product. The supernatant of the reaction mixture (90 μL) was analyzed with a reverse-phase HPLC system equipped with a fluorescence detector on a ZORBAX 300 SB-C18 4.6 mm × 150 mm column (Agilent Technologies). The fluorescence signal was monitored with excitation at 340 nm and emission at 405 nm. All peaks were integrated and normalized with the internal standard for product quantification.

Electron Microscopy. Negatively stained specimens were prepared by applying 2 μL (0.2 mg/mL) of the MBP−YqgP solution on glow-discharged carbon-coated cooper grids followed by washing and blotting with 1% uranyl acetate. Samples were examined in a JEM-1230 electron microscope (JEOL, Tokyo, Japan) at an accelerating voltage of 80 keV, and images were recorded on a 1kx1k CCD camera (Erlangshen, Gatan Inc., Pleasanton, CA).

Lipid Analysis of Purified MBP−YqgP. Lipid analysis was performed with a procedure described previously (*24*). Briefly, purified MBP−YqgP (10 μL of a 1 mg/mL solution) was mixed with 40 μL of a chloroform/methanol mixture (1:2, v/v) and spotted onto a TLC plate (silica gel 60 F254, Merck). Various amounts of total lipid extract from *E. coli* (Avanti Polar Lipids) were spotted as a positive control. After sample spots completely dried, the TLC plate was resolved in a chloroform/methanol/25% aqueous ammonia mixture (volume ratio of 65:25:5). We visualized the lipid by spraying the dried plate with 0.1% 8-anilino-1-naphthalenesulfonic acid (Sigma) under UV light.

Reconstitution of YqgP into Proteoliposomes. Medium, 100 nm unilamellar vesicles were made from mixtures of lipids using extrusion; 400 μL (3.2 mg of total lipid) of a freshly prepared batch of MUV (medium unilamellar vesicle) was mixed with 25.6 μL of a 10% CHAPS solution with a lipid:detergent ratio of 1:0.8 (w/w) followed by end-over-end rotation at 4 °C for 1 h. MBP−YqgP (0.514 mg/mL) was added to the liposome/detergent mixture at a 1:100 protein:lipid ratio (w/w) and end-over-end incubation at 4 °C for 2 h. Removal of the detergent was initiated by incubation with SM-2 beads (200−300 mg/each cycle) at 4 °C for 1 h and completed by dialysis with resuspension buffer (total 4 L) for 6 h at 4 °C. The dialysates were treated with thrombin at 16 °C for 3 h to remove the MBP tag. The YqgP proteoliposomes were incubated with substrate, and the product was analyzed by HPLC as described above.

RESULTS

High Levels of Expression of Rhomboid Can Process Spitz in the Absence of Star in Cells. Three rhomboid proteins, Rho-1 from *Drosophila*, RHBDL2 from human, and YqgP from *B. subtilis*, all of which show conservation of the catalytic dyad (Ser-His) and a highly conserved residue Asn, were selected and tagged to determine their activities (Figure 1A,B). Both rhomboid and Spitz were cotransfected with or without Star, the chaperone which is required to export Spitz to the Golgi complex where rhomboid cleaves Spitz. YqgP alone is capable of cleaving Spitz (Figure 1C, lane 3, top panel), whereas RHBDL2 and Rho-1 appear to require the presence of Star (Figure 1C, lanes 4, 5, 7, and 8, top panel). However, Star does enhance the processing of Spitz by YqgP (Figure 1C, lane 3 vs lane 6, top panel). Upon further examination of the expression of YqgP, RHBDL2, and Rho-1, we found that the level of expression of YqgP is much higher than those of the other two proteins (Figure 1C, bottom panel). We reasoned that overexpression of rhomboid overcomes the requirement of Star. To test whether Spitz cleavage is dependent on the amounts of expressed rhomboid, we enhanced the expression of rhomboid through transfection with increasing DNA input. As expected, the cleaved Spitz product was detected in the absence of Star when 1 μg of the plasmid of Rho-1 or RHBDL2 was transfected (Figure 1D). Therefore, these studies suggest that rhomboids are capable of cleaving Spitz in the absence of Star if rhomboid expression levels are sufficiently high and YqgP is a good candidate for the reconstitution of proteolytic activity.

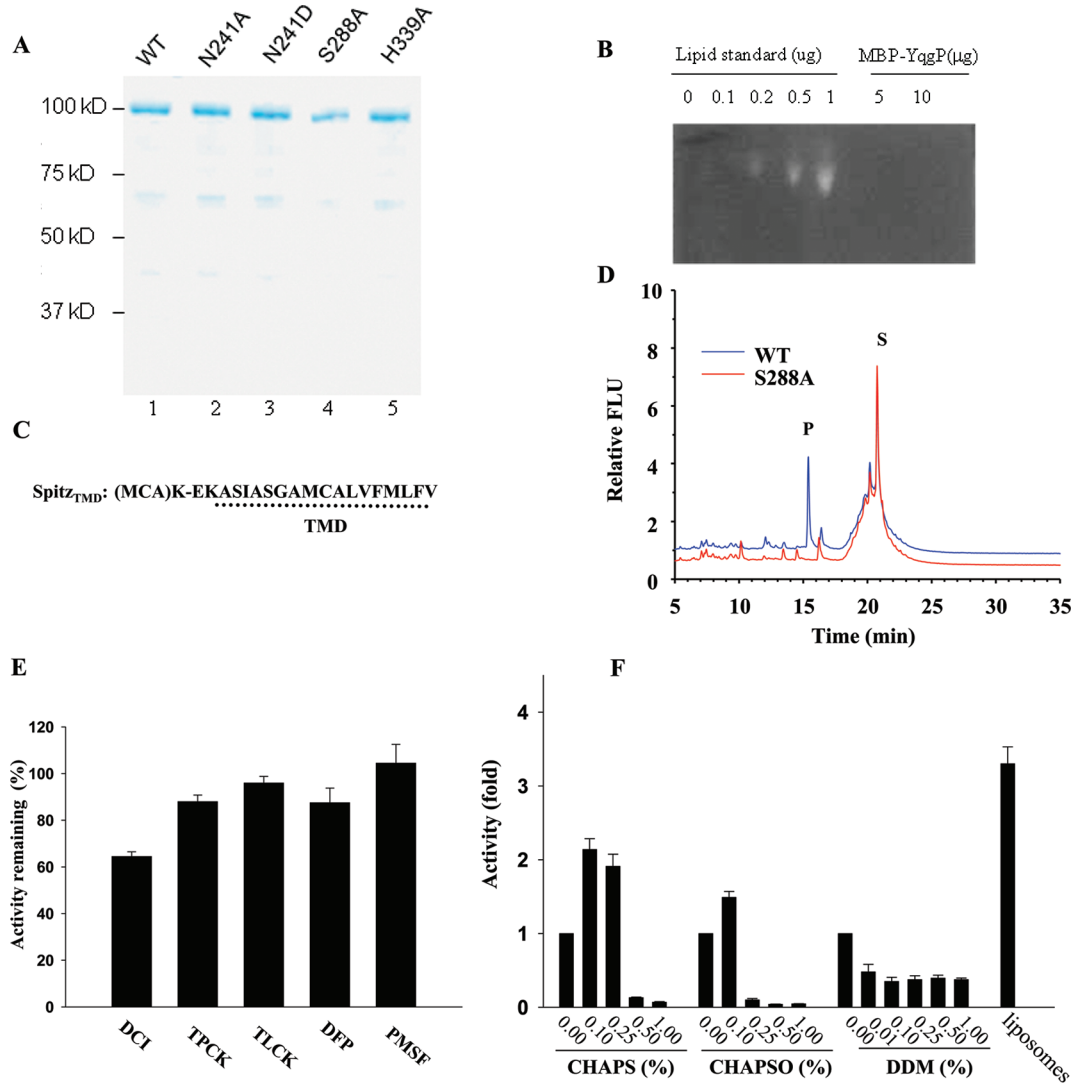

FIGURE 2: In vitro reconstitution of Spitz cleavage by YqgP. (A) Overexpression of MBP-tagged YqgP and its mutants. Purified protein was analyzed via SDS−PAGE and stained with Coomassie blue. (B) Lipid analysis. Lipid standard and purified MBP−YqgP were analyzed via thin-layer chromatography. (C) Fluorescence-labeled peptide substrate. The peptide substrate consists of the transmembrane domain (indicated by the dotted line) of Spitz and the fluorescent tag MCA, which is used to monitor the cleavage of substrate. (D) Reconstitution of in vitro MBP−YqgP activity. The reaction mixture was analyzed with a reverse-phase HPLC system equipped with a fluorescence detector (excitation at 340 nm, emission at 405 nm). The blue line represents the cleavage activity of wild-type MBP−YqgP, while the red line represents the cleavage activity of MBP−YqgP S288A (S, substrate peak; P, product peak). (E) Effects of commonly used serine protease inhibitors on the cleavage of Spitz$_{TMD}$. Each inhibitor at 400 μM was used for the cleavage assay ($n = 3$; mean ± SD). (F) Effects of detergents and liposomes on MBP−YqgP activity. MBP−YpqP activity was assayed in the absence and presence of detergents (CHAPS, CHAPSO, DDM, and Triton X-100). There was no activity in the presence of 0.1−1% Triton X-100. Effects of detergents on the cleavage were calculated as the percentage of the activity conducted without detergents (bar denoted with 0) ($n = 3$; mean ± SD).

Soluble Recombinant YqgP Is Catalytically Active. We attempted to express YqgP as a soluble protein by fusing it to the maltose binding protein (MBP). The MBP tag without signal sequence that directs target protein into membranes was fused with the YqgP protein at the N-terminus in a pIAD16 plasmid (*23*). The fusion protein was expressed in *E. coli* and isolated from the 100000*g* supernatants using an amylose column in the absence of detergent. The purified protein was analyzed by SDS−PAGE (Figure 2A, lane 1). A major protein band with a molecular mass of 100 kDa that corresponds to the fused protein of MBP−YqgP was observed (Figure 2A). Moreover, tandem mass analysis of the in-gel-digested band confirmed its identity as the MBP−YqgP protein (data not shown). Two minor bands migrate with molecular masses of 58 and 44 kDa, which were identified by LC−MS/MS as MBP with the partial N-terminal fragment of YqgP that contains no key residue of Asn, Ser, or His and as MBP, respectively. Employing the same strategy, we were able to overexpress and purify four mutant YqgP proteins, N241A, N241D, S288A, and H339A, with the same purity (Figure 2A, lanes 2−5). These MBP−YqgP proteins were isolated in high yield with approximately 2 mg from 1 L of bacterial culture. To confirm that bacterial lipids were not copurified in our protein samples, we performed lipid analyses of purified MBP−YqgP (Figure 2B). The detection limit of the assay was 0.2 μg of lipid, and even when 10 μg of purified protein was assayed, no lipid traces were detected, indicating the absence of significant amounts of lipid in our preparation.

Since YqgP cleaves Spitz to release the ligand domain for EGFR signaling, we chemically synthesized a peptide that contains the transmembrane domain of Spitz and a MCA

[(7-methoxycoumarin-4-yl)acetyl] fluorescent tag that allows for the detection and quantification of the cleaved products with high sensitivity (Figure 2C). After recombinant soluble MBP−YqgP was incubated with the peptide substrate $Spitz_{TMD}$, the reaction mixture was analyzed by a HPLC system equipped with a fluorescence detector. In addition to the substrate peak (S) eluting at 20 min, a major new peak (P) at 15.5 min was detected from the reaction mixture of MBP−YqgP and Spitz peptide (Figure 2D, WT, blue line). To rule out the possibility that this cleavage product peak (P) was produced by an unknown protease which copurified with rhomboid, the Spitz peptide was incubated with a catalytically dead mutant in which the active site nucleophile serine residue is substituted with Ala (S288A). No peak P was detected in the S288A reaction (Figure 2D, S288A, red line). Moreover, the H339A mutant in which the active site His residue was replaced with Ala led to no product formation (data not shown). These studies confirm that the cleaved product (peak P) of the Spitz peptide is derived from MBP−YqgP activity

After validating this in vitro assay, we determined the inhibitor profiles of YqgP using established serine protease inhibitors: 3,4-dichloroisocoumarin (DCI), tosyl-L-phenylalanine chloromethyl ketone (TPCK), tosyl-L-lysine chloromethyl ketone (TLCK), diisopropyl fluorophosphate (DFP), and phenylmethanesulfonyl fluoride (PMSF). DCI at a concentration of 400 μM blocks 35% of protease activity, whereas other tested inhibitors have no considerable effect (Figure 2E). Other studies suggest that DCI at 100−400 μM completely inhibits YqgP activity (*17, 18*). We reasoned that slow entrance of DCI into the active site in the presence of substrate caused a moderate inhibition. To test this notion, we have preincubated DCI with MBP−YqgP at 400 μM for 60 min and then added substrate to test the remaining protease activity. We found that DCI at 400 μM was capable of totally abolishing YqgP activity (data not shown).

Next, we examined the effect of detergents on the MBP−YqgP protease activity (Figure 2F). CHAPS at 0.1 and 0.25% stimulated MBP−YqgP activity 2.1- and 1.8-fold, respectively. However, higher concentrations (0.5 and 1.0%) significantly suppressed the protease activity (>85% inhibition). CHAPSO has a tendency similar to that of CHAPS except that it reduced activity at 0.25%. However, the presence of DDM ranging from 0.01 to 1% leads to a similar reduction in MBP−YqgP activity (40−45%). MBP−YqgP exhibits no activity in the presence of Triton X-100 (0.1−1%) (data not shown). It appears that detergents potentiated the proteolytic activity when their concentration was considerably lower than the critical micelle concentration (CMC), and they attenuated or abolished the activity when the concentration of detergents was close to or at the CMC. Subsequently, we inserted YqgP into liposomes and determined its activity. The YqgP proteoliposomes manifested 3.3-fold higher activity than soluble YqgP (Figure 2F). In other words, the specific activity of YqgP in the absence of detergent or membranes is 30% of that of YqgP when it is engaged in the lipids.

We next mapped the cleavage site through tandem MS analysis. Peak P was collected from HPLC and analyzed via Agilent LC−MS/MS. A single peak at *m*/*z* 655 was detected (Figure 3A). This peak matches the mass of the peptide MCA-KEKASIASGAM with double charges ($z = 2$, measured mass = 1308, calculated mass = 1309). A tandem mass analysis (MS/MS) of the *m*/*z* 655 mass peak detected a series of mass fragments, *m*/*z* 602.2, 673.2, 760.2, 873.3, 944.2, 1031.2, 1088.3, and 1159.3, which perfectly matched the b_3−b_{10} ions of the assigned peptide sequence, respectively (Figure 3B). This result clearly indicated that MBP−YqgP specifically cleaves the peptide bond between Met and Cys on Spitz. To further determine the role of the Met and Cys residues in substrate recognition, the two residues were separately replaced with Ala in Spitz, resulting in two mutants, M145A and C146A. Each mutation was cotransfected with YqgP in COS-1 cells to assess their effects on cleavage of Spitz by YqgP. Both substrate mutants (M145A and C146A) can still be effectively processed by YqgP-expressing cells, but not by the empty vector-expressing cells (Figure 3C). Subsequently, we synthesized peptide substrates with the M145A or C146A mutation and determined the cleavage site. HPLC analysis showed that both peptide substrates can be cleaved by MBP−YqgP as well at the same rate (data not shown). However, LC−MS analyses have revealed an extra species with a molecular mass of 1450 (*m*/*z* 726, $z = 2$) that comigrated with the *m*/*z* 1308 product in HPLC for the C146A substrate (Figure 3D). The M145A mutation caused a shift in the cleavage site toward the C-terminus by two and three residues. There are two cleaved products at *m*/*z* 1420 (*m*/*z* 711, $z = 2$) and *m*/*z* 1534 (*m*/*z* 768, $z = 2$) for the M145A substrate (Figure 3D). The identity of these species was confirmed by LC−MS/MS. Moreover, these products were not detected when each substrate was incubated with the S288A mutant (data not shown).

Finally, we compared the reactivity and specificity of the soluble form of MBP−YqgP with those of the membrane-associated one. YqgP-His6 was expressed in *E. coli* and solubilized with 1% DDM from bacterial membranes. YqgP was purified (Figure 3E) and then incubated with the $Spitz_{TMD}$ substrate, and the protease activity was analyzed as described above. A product peak (P) migrated at the same position as observed with soluble MBP−YqgP (data not shown; see Figure 2D). This peak was collected and analyzed by LC−MS/MS. Again, it appeared as a single peak at *m*/*z* 665 (data not shown). Tandem mass spectra confirmed that the exact same product was generated by both the membrane-associated form and the soluble form of YqgP. We further assessed the protease activity of soluble and membrane-associated YqgP (Figure 3F). If we normalized the protease activity of MBP−YqgP in the absence of detergent as 100%, MBP−YqgP and YqgP in the presence of DDM represent 53 and 150% of the activity, respectively. These studies indicate that soluble MBP−YqgP exhibits activity similar to that of and the same specificity as the membrane form of YqgP.

Mutations of Conserved Asn241 Significantly Reduce the Catalytic Efficiency of MBP−Yqg. In addition to Ser and His residues, classical serine proteases contain an Asp residue that forms a triad to enhance the nucleophilicity of Ser by orienting His, whereas rhomboids possess a conserved Asn residue instead. To investigate the effect of Asn on catalysis, this residue was substituted with different residues. First, we replaced Asn with Ala (N241A) and determined the kinetic parameters of YqgP proteins. Values of K_m and V_{max} are 0.70 ± 0.14 μM and 4.05 ± 0.18 pmol min^{-1} μg^{-1} for WT and

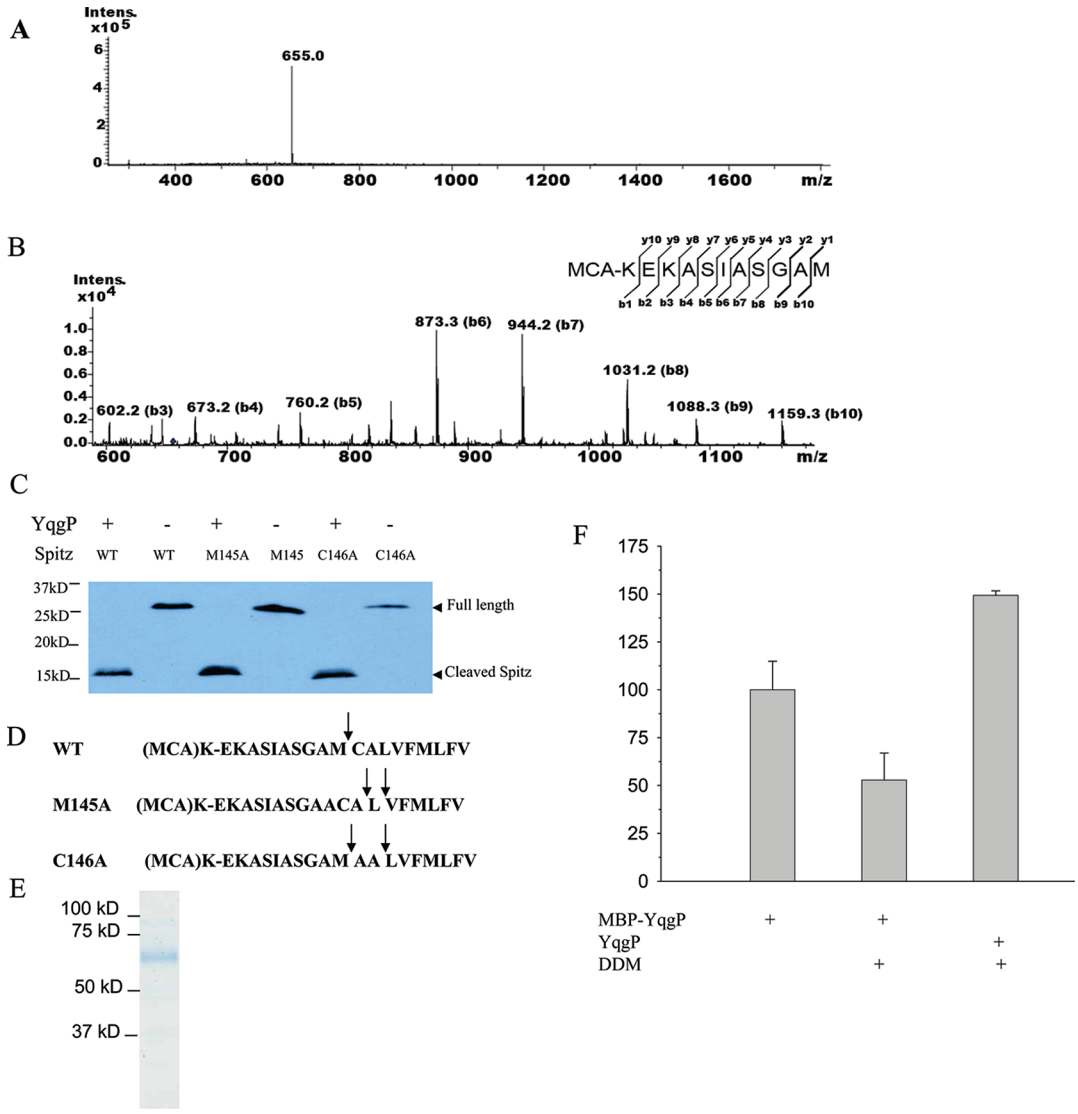

FIGURE 3: Determination of the Spitz$_{TMD}$ cleavage site by LC−MS/MS analysis. (A) The peak at 15.5 min (see Figure 2D) from reverse-phase HPLC was collected and analyzed by LC−MS/MS. A species at *m*/*z* 655 ($z = 2$) was detected. (B) LC−MS/MS spectra of the *m*/*z* 655 ($z = 2$) species. Tandem MS matched a peptide with an amino acid sequence to MCA-KEKASIASGAM (b ions are denoted in the bracket). The inset scheme shows that b and y ions arise from the Spitz$_{TMD}$ product. (C) Effects of M145A and C146A mutations on cellular YqgP activity. The Spitz WT, M145A, or C146A plasmid was cotransfected into COS-1 cells with the YqgP plasmid. After 48 h, cell lysates were analyzed by Western analysis as described in the legend of Figure 1. (D) Summary of cleavage of Spitz$_{TMD}$ by YqgP and the effect of the mutation of Met and Cys on the cleavage. Cleavage sites are denoted with arrows. (E) Analyses of YqgP isolated from membrane fractions. Purified protein was separated by SDS−PAGE and stained with Coomassie blue. (F) Comparison of the protease activity of MBP−YqgP and YqgP. The substrate Spitz$_{TMD}$ was incubated with both forms of YqgP: MBP−YqgP isolated as a soluble protein and YqgP purified from membrane fractions. The activity was determined as described in the legend of Figure 2 ($n = 3$, mean ± SD).

0.58 ± 0.18 and 0.61 ± 0.074 pmol min^{-1} μg^{-1} for N241A, respectively (Figure 4). These results suggest that replacement of Asn241 with Ala leaves the K_m unchanged but substantially reduces its V_{max} to 15% of the WT value. In other words, the N241A mutation does not affect the interaction between the substrate and protease but rather diminishes the catalytic power of the His-Ser pair. Next, we mutated Asn to Asp (N241D) to check whether Asp could restore or enhance the catalytic activity of the His-Ser dyad. The N241D mutant exhibits the same K_m (0.64 ± 0.25 μM) as WT (Figure 4). However, the V_{max} value (0.95 ± 0.06 pmol min^{-1} μg^{-1}) is 23% of that of WT and 155% of that of N241A.

Soluble MBP−YqgP Proteins Assemble into Oligomers for Catalysis. An intriguing question is how the multiple-pass transmembrane protein MBP−YqgP remains soluble and exhibits catalytic activity in the absence of detergent. Since amphiphilic molecules in aqueous solutions spontaneously form micelles or vesicles, we hypothesize that MBP−YqgP, which consists of the hydrophilic soluble domain MBP and a hydrophobic membrane protein YqgP, oligomerizes to form micellelike structures, in which MBP faces bulk water while YqgP remains in a hydrophobic environment (Figure 5A). In other words, oligomerization of YqgP leads to the formation of high-molecular mass complexes that are required for its proteolytic activity. To test this hypothesis, we initially separated the complexes by gel-filtration chromatography and determined the active fraction by using our in vitro assay (Figure 5B). There are two major peaks detected by absorbance at 280 nM (Figure 5B, red dotted line), high (H)- and low (L)-molecular mass peaks that migrate at approximately 2000 and 140 kDa, respectively.

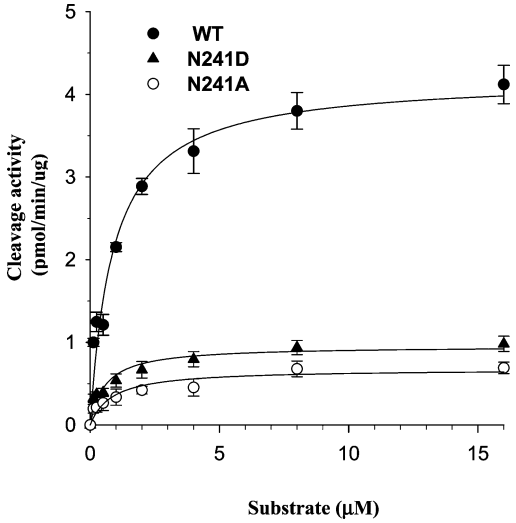

FIGURE 4: Kinetic characterization of MBP−YqgP. Determination of K_m and V_{max} of YqgP and its mutants N241D and N241A (n = 3, mean ± SD). The MBP−YqgP activity was determined at various substrate concentrations. K_m and V_{max} were calculated with the equation $V = V_{max}[S]/(K_m + [S])$.

The H peak exhibited the greatest protease activity, and the L fraction had no detectable activity. In addition, fractions with molecular masses of more than 300 kDa exhibited moderate protease activity. These studies indicate that MBP−YqgP needs to form at least a trimer for catalytic activity, and the majority of MBP−YqgP assembles into megamolecular complexes. Next, we imaged the MBP−YqgP aggregates by negative stain electron microscopy (EM). The field view displayed in Figure 5C shows MBP−YqgP complexes that are large and heterogeneous in size. It should be noted that MBP (44 kDa) has dimensions of ~30 Å × 40 Å × 65 Å, and YqgP with a molecular mass of 56 kDa should have, to a good approximation, comparable dimensions. Thus, the average size (>250 Å in any dimension) of the imaged complexes suggests that these complexes correspond to multimeric aggregates of MBP−YqgP. Remarkably, the addition of 0.1% CHAPS that augments protease activity in the sample did not have an effect on aggregate size (not shown). Next, we imaged the highly active 2000 kDa MBP−YqgP fraction after size exclusion chromatography. The eluted complexes are very homogeneous in size with average dimensions of 350 Å × 250 Å (measured from 10 individual particles) (Figure 5D). Taken together, these results suggest that the majority of MBP−YqgP aggregates into large stable multimeric structures that preserve YqgP activity. It is known that aqueous solutions generally quench fluorescence by orienting around the excited state dipoles and the partition of fluorescent molecules into detergent micelles or the membrane bilayer reduces the level of quenching (*28*). We argued that if the interior of the MBP−YqgP oligomer is hydrophobic relative to bulk water, the partitioning of a fluorescent molecule into the micellelike structure should reduce the level of water quenching. Toward this end, we examined the effect of MBP−YqgP oligomers on the fluorescence intensity of our synthetic substrate. To eliminate artifacts due to enzymatic activity, we used the catalytically dead MBP−YqgP S288A mutant. MBP−YqgP S288A or MBP was incubated with the substrate, and the fluorescence intensity was monitored. The net fluorescence intensity change was calculated by subtracting the fluorescence intensity of the fluorogenic substrate in the presence of MBP from that observed in the presence of MBP−YqgP S288A. In this experiment, MBP serves as a background control for nonspecific MBP−substrate interaction. The inset scheme shows the fluorescent signal of MBP, substrate, or enzyme alone at different time points. The difference in net fluorescent change between MBP−YqgP and MBP is attributed to the partitioning of the substrate into rhomboid oligomers (Figure 5E). These studies provide additional lines of evidence suggesting that the MBP−YqgP oligomers form micellelike catalytically competent structures.

DISCUSSION

Intramembrane proteases are polytopic membrane proteins that cleave substrates within the transmembrane domain, an apparently hydrophobic environment. Rhomboid, an intramembrane serine protease, plays a pivotal role in cellular signaling. In this work, we developed an expression system that allows production of highly purified MBP−YqgP as a soluble protein in the absence of detergents. Surprisingly, soluble MBP−YqgP is capable of cleaving a peptide substrate derived from Spitz protein. Moreover, this system allows kinetic characterization of YqgP and elucidation of the reaction mechanism in detail. Finally, we have demonstrated that soluble MBP−YqgP forms oligomers or megamolecular multimers, suggesting these functional aggregates may mimic the micellelike environments required for peptide hydrolysis.

Biochemical reconstitution of bacterial S2P (RseP or YaeL) and rhomboids (YqgP from *B. subtilis* and GlpG from *E. coli*) has been reported (*17, 18, 25*). All recombinant proteins were solubilized from the bacterial membrane and purified for reconstitution. In vitro protease activity was detected by either Western blotting (*25*) or autoradiography (*18*). Our system expresses purified MBP−YqgP as a soluble protein without the requirement of detergent. Soluble MBP−YqgP exhibits protease activity for hydrolysis of the Spitz peptide substrate. Importantly, this activity is abolished by mutation of the key catalytic residues Ser (S288A) and His (H339A) and inhibited by DCI, which was corroborated with previous reconstitution studies using membrane-solubilized YqgP (*17, 18*). Taken together, these studies have established that the cleavage activity is attributed to the recombinant YqgP, rather than contaminated soluble proteases copurified with the target protein. The next critical question is how active the soluble YqgP aggregates are compared with YqgP in the solubilized states or membranes. We have demonstrated that soluble MBP−YqgP exhibited comparable protease activity (70%) as membrane-solubilized YqgP. In addition, although there are no kinetic or enzymatic rate data from other reconstitution systems allowing for a direct comparison to soluble YqgP, the fraction (40−80%) of conversion of substrate to product by the soluble YqgP is similar to that in solubilized YqgP (*18*) after normalization for the enzyme concentration and incubation times. A low rate of turnover of solubilized intramembrane proteases has been observed in rhomboids (*18*) and γ-secretase (V_{max} = 11.8 pmol/min) (*26*). These studies suggest the soluble YqgP exhibits reasonable protease activity in the absence of detergent and membranes.

LC−MS/MS analysis mapped the cleavage site between Met and Cys, which is close to the estimated processing site

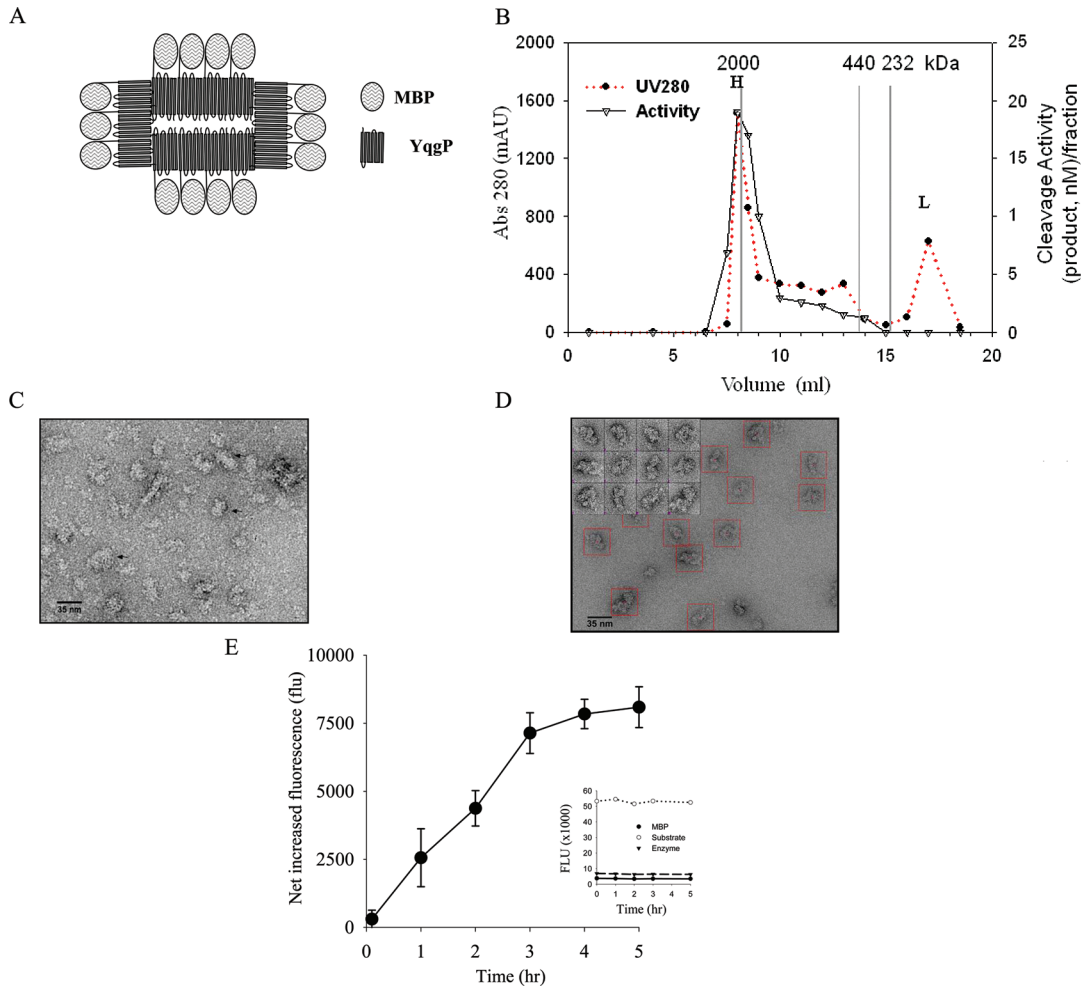

FIGURE 5: MBP−YqgP exists as oligomer or multimer complexes. (A) Hypothetical model of the megacomplex of MBP−YqgP. The hydrophilic MBP part faces outside, while the hydrophobic YqgP is buried inside. (B) Comigration of MBP−YqgP protein complexes and protease activity during gel exclusion chromatography. Purified MBP−YqgP was chromatographed with a Superose6 gel-filtration column. The A_{280} profile of the eluent is shown (dotted line). Fractions were collected and assayed for MBP−YqgP activity. (C) Electron microscopy image of negatively stained MBP−YqgP before size exclusion chromatography in the absence of detergent. The MBP−YqgP aggregates (marked by black arrows) are quite heterogeneous in size. (D) Electron microscopy image of negatively stained MBP−YqgP eluted via size exclusion chromatography (SEC) with an apparent molecular mass of 2000 kDa. After SEC, the MBP−YqgP aggregates are homogeneous in size with average dimensions of ~350 Å × 250 Å. The inset shows individual boxed particles. The scale bars correspond to 35 nm. (E) Fluorescence changes resulted from interaction between the substrate and the MBP−YqgP complex. MBP−YqgP S288A or MBP (1 μM) was incubated with 8 μM fluorescent substrate, and the fluorescent signals were monitored (excitation at 340 nm, emission at 405 nm). Substrate, MBP, or MBP−YqgP alone was used for background correction. After background had been subtracted, the difference (Δ = MBP−YqgP − MBP) was used as an index of the substrate and enzyme interaction (*Y*-axis). The inset shows the fluorescent signal of MBP, substrate, or enzyme alone at different time points.

from cellular studies (*7*). This work has illustrated that the transmembrane domain of Spitz is sufficient to serve as a substrate for MBP−YqgP, which is consistent with cellular and biochemical studies (*18, 27*). Importantly, we have demonstrated that soluble MBP−YqgP possesses the same specificity as membrane-associated YqgP. Furthermore, replacement of Met145 or Cys146 with Ala in Spitz led to the generation of additional or alternative cleavage sites. If these peptides are considered to form α-helical structure, which is a favorable conformation that the transmembrane domains tend to fold (*28*), these cleavage sites would be located in different faces of the helix (Figure 6). The C146A mutation allows the protease to access scissile bonds from opposite directions, whereas the M145A mutation results in generation of two novel cleavage sites on the Spitz substrate. How these mutations affect the conformation of substrates and lead to the alternation of interaction between substrate and protease requires more biophysical and structural studies. These findings support the notion that the major determinant of specificity for rhomboid is the conformation of the substrate, rather than the primary sequence (*27*). It has been reported that GlpG cleaves both Ala−Ser and Gly−Ala bonds in a hybrid substrate in which the first seven residues of the amyloid precursor protein (APP) transmembrane domain were replaced with the corresponding Spitz peptide (ASIASGA) (*17, 29*) that is recognized by rhomboid (*27*). Whether distinct cleavage sites result from different substrates and/or different rhomboids remains to be investigated. Multiple cleavage sites have been observed in γ-secretase for APP and Notch processing (*30*).

Cellular mutagenesis studies suggested that rhomboid could contain an Asn-His-Ser triad for catalysis (*7*). However, structural studies have demonstrated that Asn is not proximate to the Ser-His pair for hydrogen bonding to stabilize the His residue. Therefore, rhomboid belongs to a class of dyad serine hydrolases (*19, 20*) in which the His-Ser ion

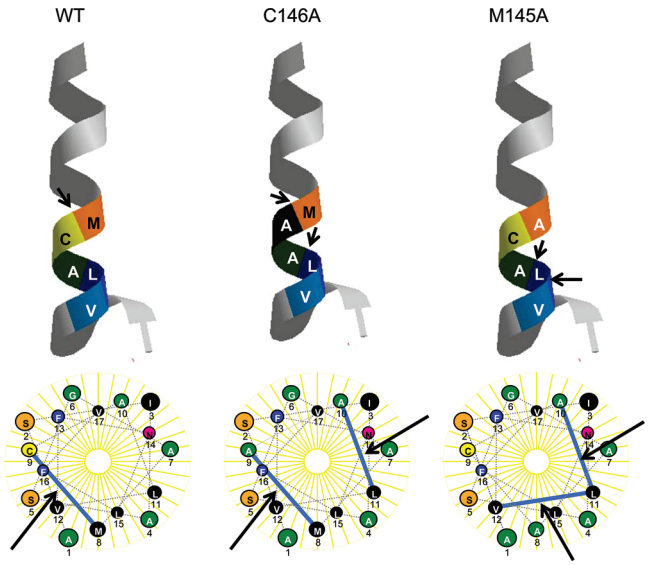

FIGURE 6: Helical models of peptide substrate and cleavage sites. The helical wheel was modeled with Lasergene 6. The cleavage sites in the WT, C146A, and M145A substrates are denoted with arrows.

pair is capable of performing effective catalysis. The side chain of Asn is likely involved in the formation of the oxyanion hole to enhance catalysis (*31*). However, mutation of Asn residue did not affect in vitro YqgP activity (*18*), which is in contrast to cellular studies in which Asn mutations considerably reduced and blocked rhomboid protease activity (*32*). N241A and N241D mutations in this study resulted in reductions in the catalytic efficiency of MBP−YqgP of 6- and 4-fold, respectively. If Asn is one of the catalytic residues, it was expected that the effect of these mutations on the rate would be much more dramatic ($>10^3$-fold), such as the effects of trypsin (*33*) and subtilisin (*34*) in which the catalytic Asp was replaced with Ala. In this regard, MBP−YqgP is more closely related to the outer membrane phospholipase (OMPLA) that is an integral membrane enzyme with conserved Asn-His-Ser residues (*35*). Replacement of Asn with Ala and Asp in OMPLA led to 20- and 2-fold decreases in activity, respectively (*36*). We have also demonstrated that these mutations have no effect on the interaction of the substrate protease but affect the catalytic power. Taken together, these findings indicate that Asn does not directly contribute to catalysis but plays a critical role in rhomboid activity, which is corroborated by previous conclusions from structural and cellular studies (*19*−*21, 29, 32*).

Our study has shown that soluble MBP−YqgP proteins form oligomers or multimers for catalysis. Stable trimers or multimers of rhomboid have been observed in other studies (*18, 20*). In addition, the formation of oligomers has been observed in other intramembrane proteases, such as γ-secretase (*37, 38*) and SPP (*39, 40*). We demonstrated that γ-secretase activity is associated with the PS1-containing macromolecular complex with an apparent molecular mass of ~2000 kDa (*41*). Gu et al. (*42*) detected two γ-secretase macromolecular complexes with molecular masses of ~440 and ≥670 kDa. The higher-molecular mass complex may be oligomers of the γ-secretase complex. It is apparent that intramembrane proteases commonly form oligomers, at least in solubilized states, and the oligomers′ function in proteolysis may be related to the extraordinary catalysis of these intramembrane proteases. Their roles under physiological conditions remain to be investigated.

MBP has been proven to be a valuable tag in assisting soluble protein expression and isolation (*43*). However, when MBP was utilized for the expression of membrane proteins with multiple transmembrane domains, solubilization and refolding were needed to yield functional proteins (*43*−*45*). This experimental system allows us to directly generate soluble protein without the requirement of detergents. More importantly, this soluble fusion membrane protein (MBP−YqgP) is functionally active in the absence of detergent. Therefore, in addition to providing a practical system for studying rhomboid enzymology, this system may also be applicable for other intramembrane proteases. Whether this system can be utilized to express and isolate certain membrane proteins in soluble form and investigate their structure and function remains to be tested. Furthermore, purified MBP−YqgP can be utilized for reconstitution studies with detergents and/or lipids.

In summary, we successfully overexpressed MBP−YqgP in a soluble form without detergents and reconstituted rhomboid cleavage in an in vitro system. This assay could be an important tool for characterization of rhomboid proteases. Furthermore, our system could be used as an experimental system to characterize other intramembrane proteases as well as other membrane proteins.

ACKNOWLEDGMENT

We thank Lisa Placanica and Christopher C. Shelton for critical reading of the manuscript, Dr. Christopher T. Walsh for the pIAD16 plasmid, and Dr. Matthew Freeman for rhomboid and Spitz-1 constructs. We also thank the New York Structural Biology Center for electron microscope access.

REFERENCES

1. Brown, M. S., Ye, J., Rawson, R. B., and Goldstein, J. L. (2000) Regulated intramembrane proteolysis: A control mechanism conserved from bacteria to humans. *Cell 100*, 391–398.
2. Wolfe, M. S., and Kopan, R. (2004) Intramembrane proteolysis: Theme and variations. *Science 305*, 1119–1123.
3. Rawson, R. B., Zelenski, N. G., Nijhawan, D., Ye, J., Sakai, J., Hasan, M. T., Chang, T. Y., Brown, M. S., and Goldstein, J. L. (1997) Complementation cloning of S2P, a gene encoding a putative metalloprotease required for intramembrane cleavage of SREBPs. *Mol. Cell 1*, 47–57.
4. Wolfe, M. S., Xia, W., Ostaszewski, B. L., Diehl, T. S., Kimberly, W. T., and Selkoe, D. J. (1999) Two transmembrane aspartates in presenilin-1 required for presenilin endoproteolysis and γ-secretase activity. *Nature 398*, 513–517.
5. Weihofen, A., Binns, K., Lemberg, M. K., Ashman, K., and Martoglio, B. (2002) Identification of signal peptide peptidase, a presenilin-type aspartic protease. *Science 296*, 2215–2218.
6. Li, Y. M., Xu, M., Lai, M. T., Huang, Q., Castro, J. L., DiMuzio-Mower, J., Harrison, T., Lellis, C., Nadin, A., Neduvelil, J. G., Register, R. B., Sardana, M. K., Shearman, M. S., Smith, A. L., Shi, X. P., Yin, K. C., Shafer, J. A., and Gardell, S. J. (2000) Photoactivated γ-secretase inhibitors directed to the active site covalently label presenilin 1. *Nature 405*, 689–694.
7. Urban, S., Lee, J. R., and Freeman, M. (2001) *Drosophila* rhomboid-1 defines a family of putative intramembrane serine proteases. *Cell 107*, 173–182.
8. Rawson, R. B. (2002) Regulated intramembrane proteolysis: From the endoplasmic reticulum to the nucleus. *Essays Biochem. 38*, 155–168.

9. Bier, E., Jan, L. Y., and Jan, Y. N. (1990) rhomboid, a gene required for dorsoventral axis establishment and peripheral nervous system development in *Drosophila melanogaster*. *Genes Dev. 4*, 190–203.
10. Lee, J. R., Urban, S., Garvey, C. F., and Freeman, M. (2001) Regulated intracellular ligand transport and proteolysis control EGF signal activation in *Drosophila*. *Cell 107*, 161–171.
11. Koonin, E. V., Makarova, K. S., Rogozin, I. B., Davidovic, L., Letellier, M. C., and Pellegrini, L. (2003) The rhomboids: A nearly ubiquitous family of intramembrane serine proteases that probably evolved by multiple ancient horizontal gene transfers. *Genome Biol. 4*, R19.
12. Rather, P. N., Ding, X., Baca-DeLancey, R. R., and Siddiqui, S. (1999) *Providencia stuartii* genes activated by cell-to-cell signaling and identification of a gene required for production or activity of an extracellular factor. *J. Bacteriol. 181*, 7185–7191.
13. McQuibban, G. A., Saurya, S., and Freeman, M. (2003) Mitochondrial membrane remodelling regulated by a conserved rhomboid protease. *Nature 423*, 537–541.
14. Brossier, F., Jewett, T. J., Sibley, L. D., and Urban, S. (2005) A spatially localized rhomboid protease cleaves cell surface adhesins essential for invasion by Toxoplasma. *Proc. Natl. Acad. Sci. U.S.A. 102*, 4146–4151.
15. Cipolat, S., Rudka, T., Hartmann, D., Costa, V., Serneels, L., Craessaerts, K., Metzger, K., Frezza, C., Annaert, W., D′Adamio, L., Derks, C., Dejaegere, T., Pellegrini, L., D′Hooge, R., Scorrano, L., and De Strooper, B. (2006) Mitochondrial rhomboid PARL regulates cytochrome c release during apoptosis via OPA1-dependent cristae remodeling. *Cell 126*, 163–175.
16. Stevenson, L. G., Strisovsky, K., Clemmer, K. M., Bhatt, S., Freeman, M., and Rather, P. N. (2007) Rhomboid protease AarA mediates quorum-sensing in *Providencia stuartii* by activating TatA of the twin-arginine translocase. *Proc. Natl. Acad. Sci. U.S.A. 104*, 1003–1008.
17. Urban, S., and Wolfe, M. S. (2005) Reconstitution of intramembrane proteolysis in vitro reveals that pure rhomboid is sufficient for catalysis and specificity. *Proc. Natl. Acad. Sci. U.S.A. 102*, 1883–1888.
18. Lemberg, M. K., Menendez, J., Misik, A., Garcia, M., Koth, C. M., and Freeman, M. (2005) Mechanism of intramembrane proteolysis investigated with purified rhomboid proteases. *EMBO J. 24*, 464–472.
19. Wu, Z., Yan, N., Feng, L., Oberstein, A., Yan, H., Baker, R. P., Gu, L., Jeffrey, P. D., Urban, S., and Shi, Y. (2006) Structural analysis of a rhomboid family intramembrane protease reveals a gating mechanism for substrate entry. *Nat. Struct. Mol. Biol. 13*, 1084–1091.
20. Wang, Y., Zhang, Y., and Ha, Y. (2006) Crystal structure of a rhomboid family intramembrane protease. *Nature 444*, 179–180.
21. Lemieux, M. J., Fischer, S. J., Cherney, M. M., Bateman, K. S., and James, M. N. (2007) The crystal structure of the rhomboid peptidase from *Haemophilus influenzae* provides insight into intramembrane proteolysis. *Proc. Natl. Acad. Sci. U.S.A. 104*, 750–754.
22. Ben-Shem, A., Fass, D., and Bibi, E. (2007) Structural basis for intramembrane proteolysis by rhomboid serine proteases. *Proc. Natl. Acad. Sci. U.S.A. 104*, 462–466.
23. McCafferty, D. G., Lessard, I. A., and Walsh, C. T. (1997) Mutational analysis of potential zinc-binding residues in the active site of the enterococcal D-Ala-D-Ala dipeptidase VanX. *Biochemistry 36*, 10498–10505.
24. Butler, P. J., Ubarretxena-Belandia, I., Warne, T., and Tate, C. G. (2004) The *Escherichia coli* multidrug transporter EmrE is a dimer in the detergent-solubilised state. *J. Mol. Biol. 340*, 797–808.
25. Akiyama, Y., Kanehara, K., and Ito, K. (2004) RseP (YaeL), an *Escherichia coli* RIP protease, cleaves transmembrane sequences. *EMBO J. 23*, 4434–4442.
26. Fraering, P. C., Ye, W., Strub, J.-M., Dolios, G., LaVoie, M. J., Ostaszewski, B. L., van Dorsselaer, A., Wang, R., Selkoe, D. J., and Wolfe, M. S. (2004) Purification and characterization of the human γ-secretase complex. *Biochemistry 43*, 9774–9789.
27. Urban, S., and Freeman, M. (2003) Substrate specificity of rhomboid intramembrane proteases is governed by helix-breaking residues in the substrate transmembrane domain. *Mol. Cell 11*, 1425–1434.
28. Ubarretxena-Belandia, I., and Engelman, D. M. (2001) Helical membrane proteins: Diversity of functions in the context of simple architecture. *Curr. Opin. Struct. Biol. 11*, 370–376.
29. Baker, R. P., Young, K., Feng, L., Shi, Y., and Urban, S. (2007) Enzymatic analysis of a rhomboid intramembrane protease implicates transmembrane helix 5 as the lateral substrate gate. *Proc. Natl. Acad. Sci. U.S.A. 104*, 8257–8262.
30. Okochi, M., Steiner, H., Fukumori, A., Tanii, H., Tomita, T., Tanaka, T., Iwatsubo, T., Kudo, T., Takeda, M., and Haass, C. (2002) Presenilins mediate a dual intramembranous γ-secretase cleavage of Notch-1. *EMBO J. 21*, 5408–5416.
31. Ha, Y. (2007) Structural principles of intramembrane proteases. *Curr. Opin. Struct. Biol. 17*, 405–411.
32. Urban, S., Schlieper, D., and Freeman, M. (2002) Conservation of intramembrane proteolytic activity and substrate specificity in prokaryotic and eukaryotic rhomboids. *Curr. Biol. 12*, 1507–1512.
33. Sprang, S., Standing, T., Fletterick, R. J., Stroud, R. M., Finer-.Moore, J., Xuong, N. H., Hamlin, R., Rutter, W. J., and Craik, C. S. (1987) The three-dimensional structure of Asn102 mutant of trypsin: Role of Asp102 in serine protease catalysis. *Science 237*, 905–909.
34. Carter, P., and Wells, J. A. (1988) Dissecting the catalytic triad of a serine protease. *Nature 332*, 564–568.
35. Snijder, H. J., Ubarretxena-Belandia, I., Blaauw, M., Kalk, K. H., Verheij, H. M., Egmond, M. R., Dekker, N., and Dijkstra, B. W. (1999) Structural evidence for dimerization-regulated activation of an integral membrane phospholipase. *Nature 401*, 717–721.
36. Kingma, R. L., Fragiathaki, M., Snijder, H. J., Dijkstra, B. W., Verheij, H. M., Dekker, N., and Egmond, M. R. (2000) Unusual catalytic triad of *Escherichia coli* outer membrane phospholipase A. *Biochemistry 39*, 10017–10022.
37. Schroeter, E. H., Ilagan, M. X., Brunkan, A. L., Hecimovic, S., Li, Y. M., Xu, M., Lewis, H. D., Saxena, M. T., De Strooper, B., Coonrod, A., Tomita, T., Iwatsubo, T., Moore, C. L., Goate, A., Wolfe, M. S., Shearman, M., and Kopan, R. (2003) A presenilin dimer at the core of the γ-secretase enzyme: Insights from parallel analysis of Notch 1 and APP proteolysis. *Proc. Natl. Acad. Sci. U.S.A. 100*, 13075–13080.
38. Herl, L., Lleo, A., Thomas, A. V., Nyborg, A. C., Jansen, K., Golde, T. E., Hyman, B. T., and Berezovska, O. (2006) Detection of presenilin-1 homodimer formation in intact cells using fluorescent lifetime imaging microscopy. *Biochem. Biophys. Res. Commun. 340*, 668–674.
39. Nyborg, A. C., Kornilova, A. Y., Jansen, K., Ladd, T. B., Wolfe, M. S., and Golde, T. E. (2004) Signal peptide peptidase forms a homodimer that is labeled by an active site-directed γ-secretase inhibitor. *J. Biol. Chem. 279*, 15153–15160.
40. Nyborg, A. C., Herl, L., Berezovska, O., Thomas, A. V., Ladd, T. B., Jansen, K., Hyman, B. T., and Golde, T. E. (2006) Signal peptide peptidase (SPP) dimer formation as assessed by fluorescence lifetime imaging microscopy (FLIM) in intact cells. *Mol. Neurodegener. 1*, 16.
41. Li, Y. M., Lai, M. T., Xu, M., Huang, Q., DiMuzio-Mower, J., Sardana, M. K., Shi, X. P., Yin, K. C., Shafer, J. A., and Gardell, S. J. (2000) Presenilin 1 is linked with γ-secretase activity in the detergent solubilized state. *Proc. Natl. Acad. Sci. U.S.A. 97*, 6138–6143.
42. Gu, Y., Sanjo, N., Chen, F., Hasegawa, H., Petit, A., Ruan, X., Li, W., Shier, C., Kawarai, T., Schmitt.Ulms, G., Westaway, D., St George-Hyslop, P., and Fraser, P. E. (2004) The presenilin proteins are components of multiple membrane-bound complexes that have different biological activities. *J. Biol. Chem. 279*, 31329–31336.
43. Wang, D. N., Safferling, M., Lemieux, M. J., Griffith, H., Chen, Y., and Li, X. D. (2003) Practical aspects of overexpressing bacterial secondary membrane transporters for structural studies. *Biochim. Biophys. Acta 1610*, 23–36.
44. Chen, G. Q., and Gouaux, J. E. (1996) Overexpression of bacterioopsin in *Escherichia coli* as a water-soluble fusion to maltose binding protein: Efficient regeneration of the fusion protein and selective cleavage with trypsin. *Protein Sci. 5*, 456–467.
45. Korepanova, A., Moore, J. D., Nguyen, H. B., Hua, Y., Cross, T. A., and Gao, F. (2007) Expression of membrane proteins from *Mycobacterium tuberculosis* in *Escherichia coli* as fusions with maltose binding protein. *Protein Expression Purif. 53*, 24–30.

BI800385R